Group of
Particle Physics and Astrophysics

Department of Physics
University of Tirana

Science Week,
20-24 November 2023,
Tirana

Prof. Mimoza Hafizi
Prof. As. Lindita Hamolli
Prof. As. Rudina Osmanaj
Dr. Sonila Boçi
Dr. Ervin Kafexhiu

I. Lattice QCD

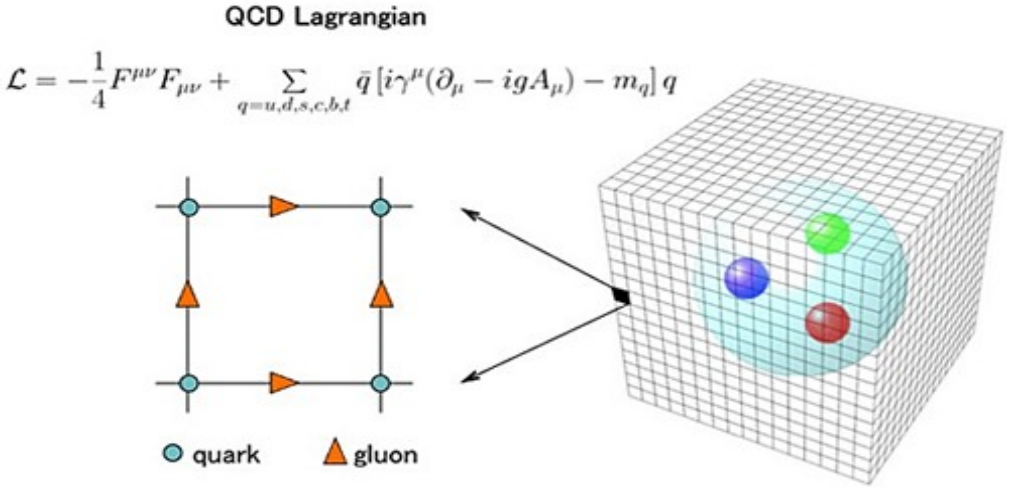

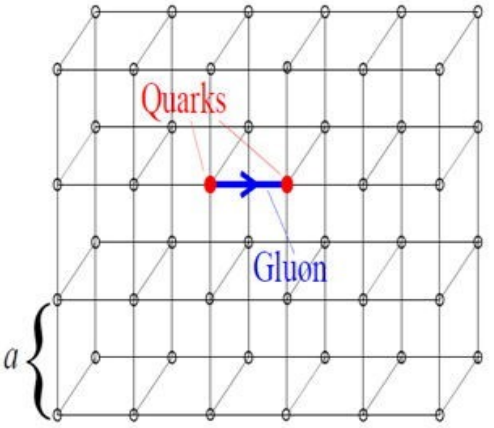

- Chiral fermions on the lattice - Minimally doubled fermions *(Osmanaj Talk)*

  - Properties of minimally doubled fermions (Open collaborations with University of Wuppertal, Julich Supercomputing Center, Humboldt University)

  - Simulations with MDF in Lattice QCD (as possible "candidate" fermions to be used widely by the LQCD community)

- Krylov subspace methods in lattice QCD – Inversion algorithms

I. Lattice QCD: Effects of the broken hyper-cubic symmetry on the light hadrons spectrum

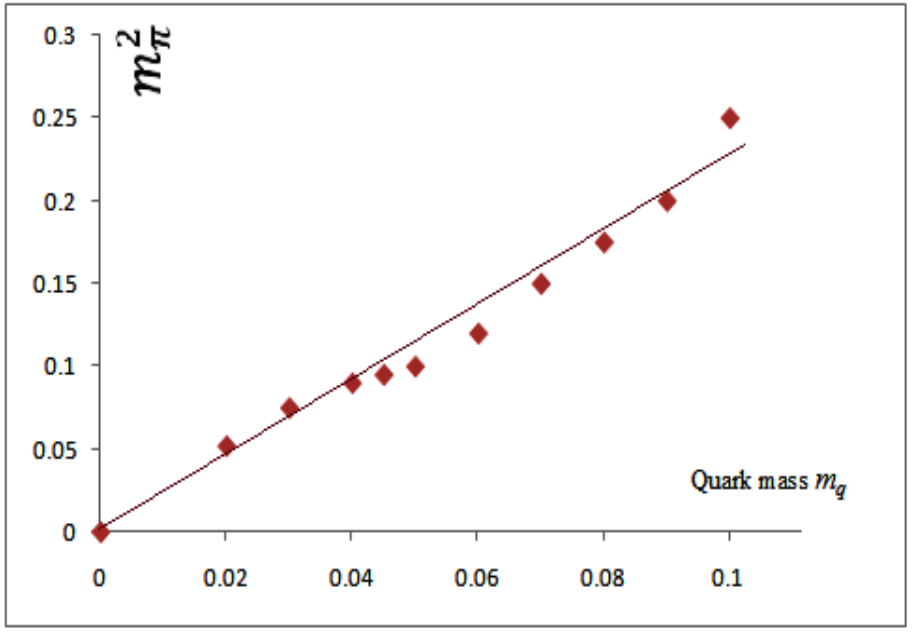

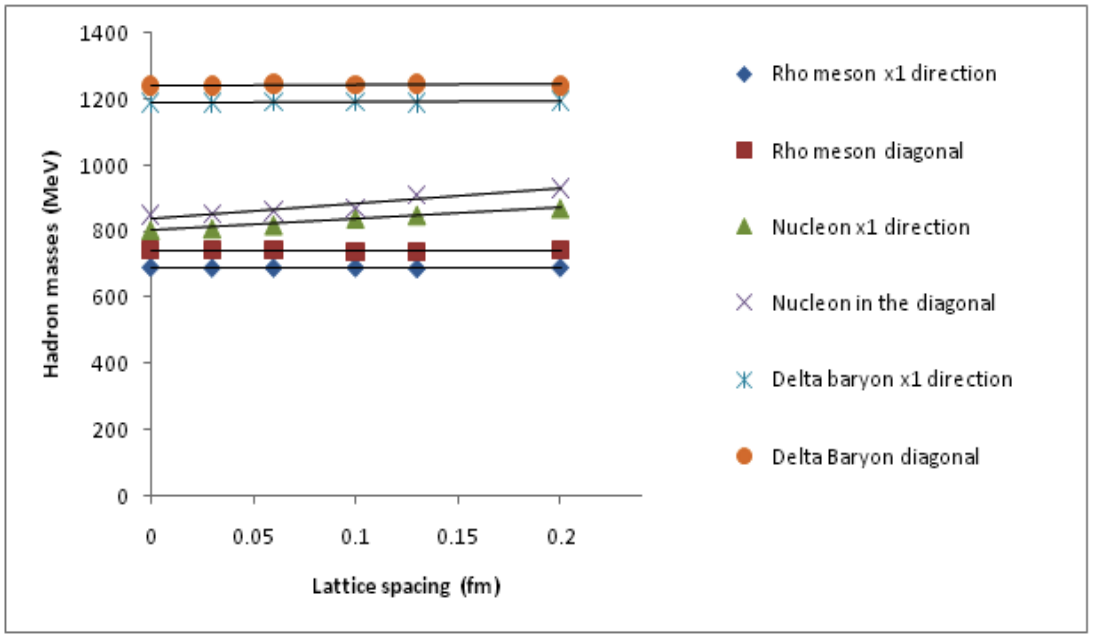

- Quenched approximation
- BC fermionic action
- Wilson gauge action
- 500 configurations

- Point source for quark propagators
- BiCGstab inverter
- Point splitting method
- FermiQCD

I. Lattice QCD: Light hadrons masses

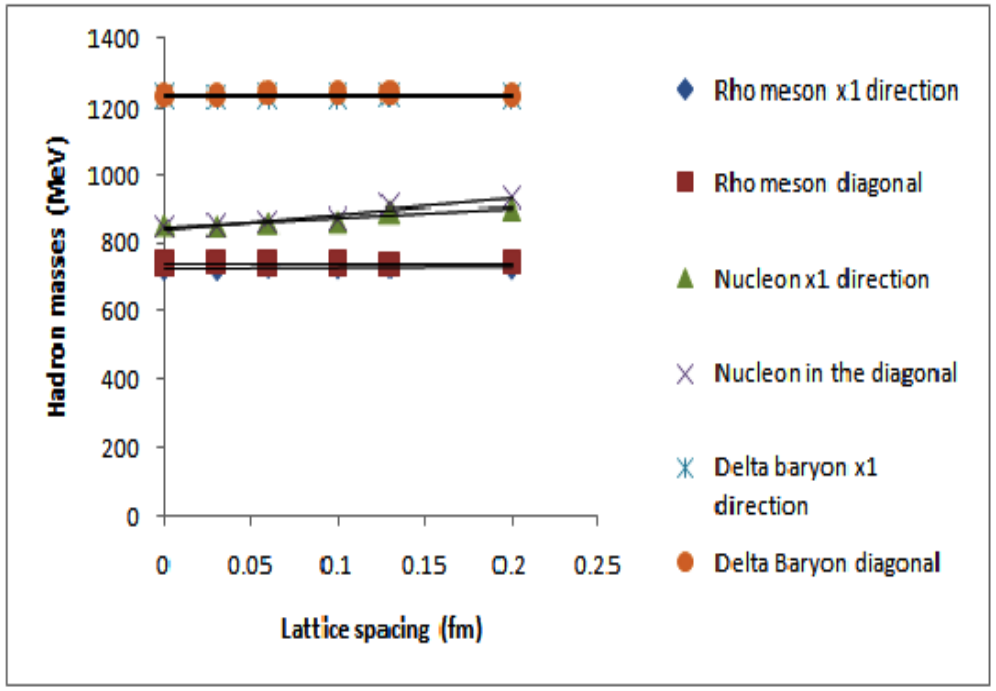

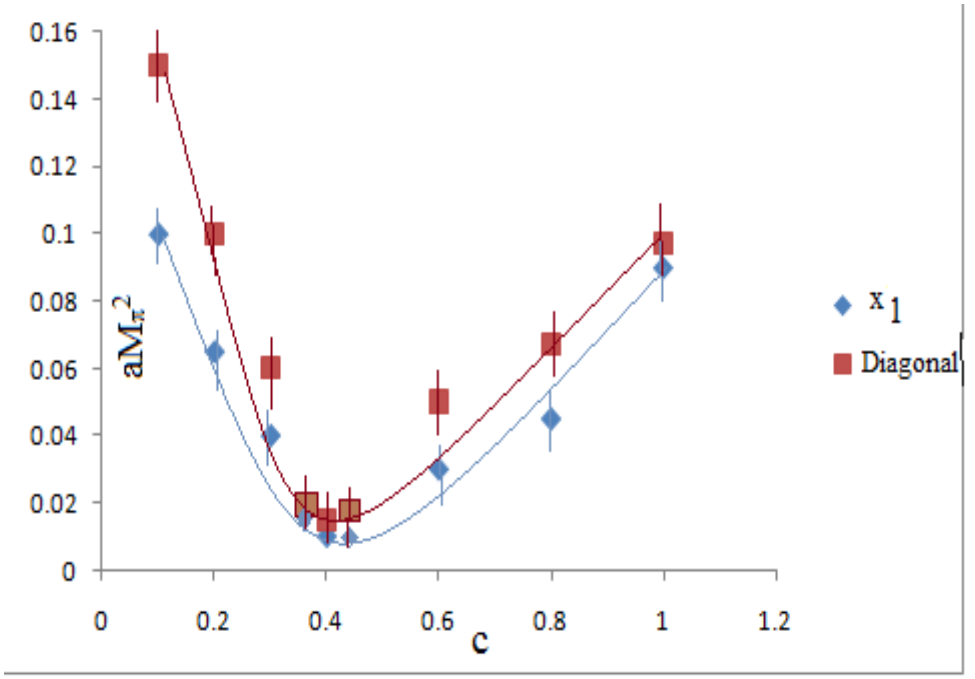

Hadron	Masses using the diagonal (MeV/c2)	Masses using the x1 direction(MeV/c2)
Rho - meson	741	690
Nucleon	849	805
Delta	1240	1187

BC without adding c_3

Hadron	Masses using the diagonal (MeV/c2)	Masses using the x1 direction(MeV/c2)
Rho - meson	741	730
Nucleon	860	852
Delta	1240	1236

Corrected BC by adding c_3

I. Lattice QCD: Inversion Algorithms - Results

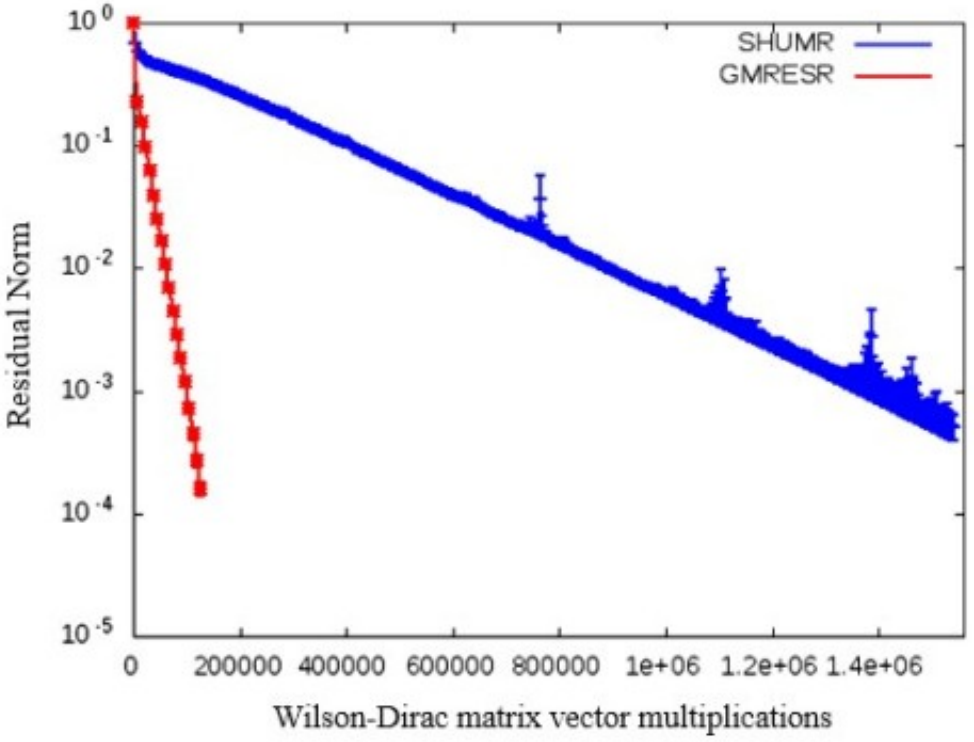

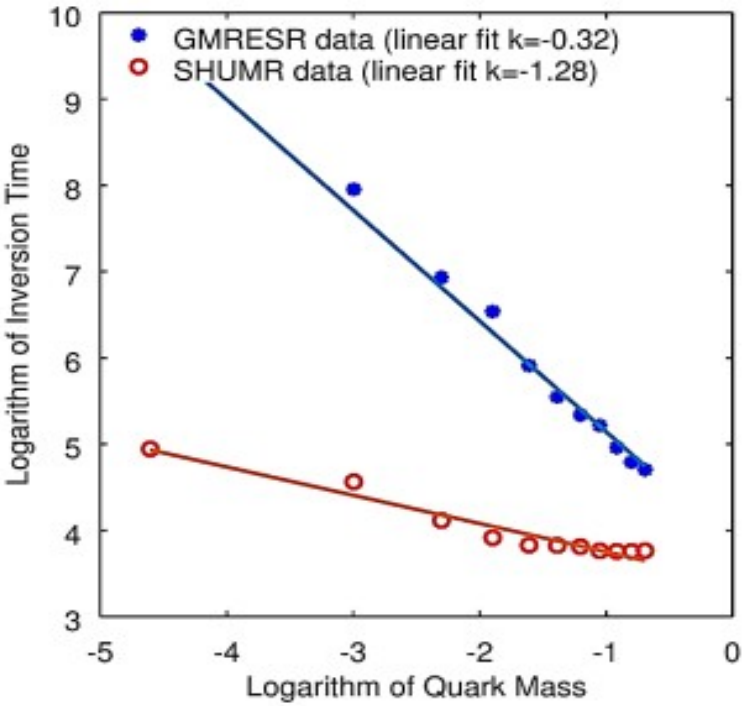

II. GRAVITATIONAL LENSING

A light ray from a distant source passes close to a mass distribution is bent. General Relativity (Einstein, 1916) predicted an angle 2x larger than Newtonian Gravity.

- **Deflection angle** $\vec{\hat{\alpha}}(\vec{\xi}) = \frac{2}{c^2}\int \vec{\nabla}_\perp \Phi(\vec{\xi}, z)dz$

- **The lens equation is found to be (*Einstein, 1936*)**

$$\vec{\theta} - \vec{\beta} = \alpha(\vec{\theta}) \qquad \vec{\beta} = 0$$

$$\vec{\alpha}(\vec{\theta}) = \frac{D_{LS}}{D_S}\vec{\hat{\alpha}}(\vec{\theta}) \qquad \theta_E = \sqrt{\frac{4GM(\theta)}{c^2}\frac{D_{LS}}{D_S D_L}}$$

- **D_L, D_S & D_{LS} are the angular diameter distances observer-source, observer-lens and lens-source**

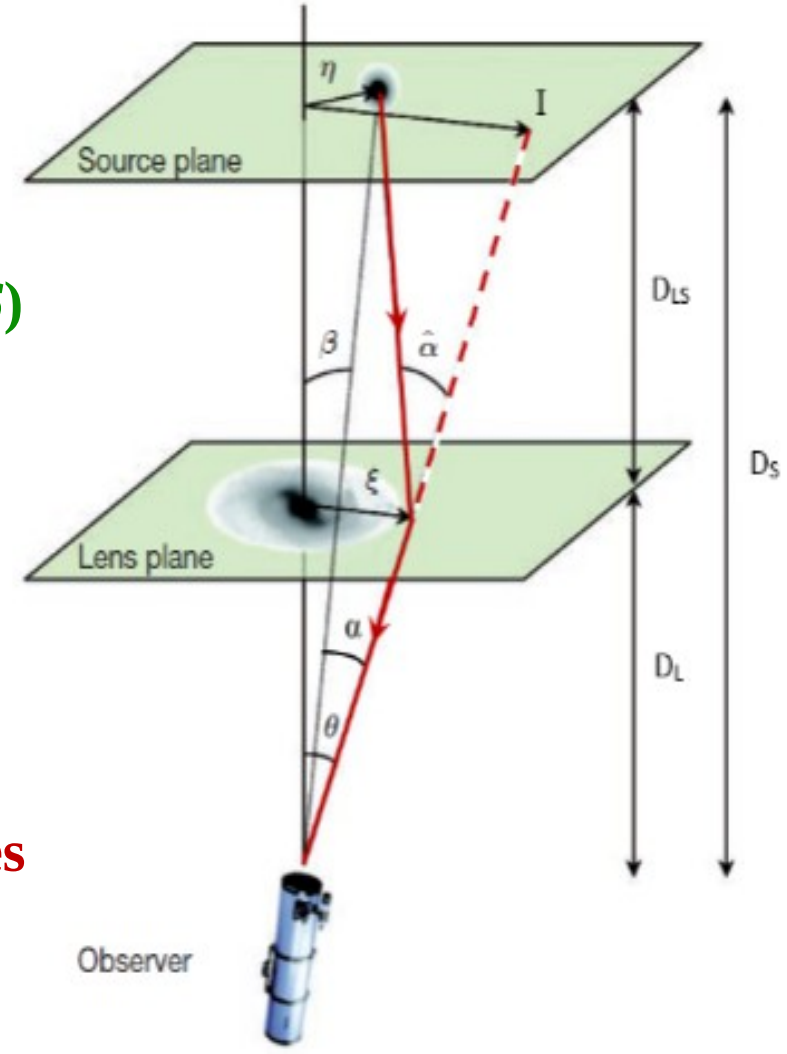

II. GRAVITATIONAL LENSING: Three Classes of lensing

A) **Strong lensing. High distortions, Einstein rings, arcs and multiple images separated by several arcsecs** ***(Galaxy Cluster SDSS J1004+4112, HST).***

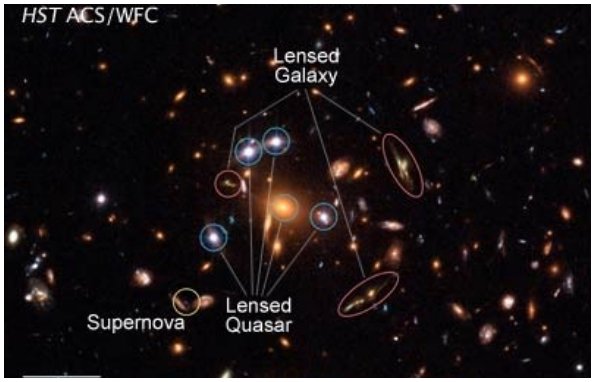

B) **Weak lensing**. Much smaller distortions due to large angular separations of the lensing galaxies or galaxy clusters to the line of sight **("Topographical map" of the dark matter in the Bullet Cluster, detected using weak lensing, Miyazaki et al., 2015).**

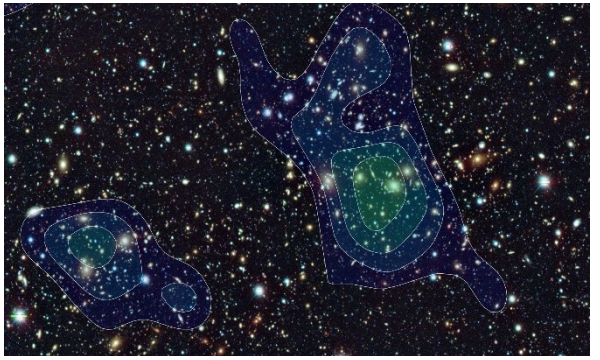

C) **Microlensing**. No visible distortions, but a variable magnification of the source light ***(Paczynski, 1986).*** Small mass lenses **($10^{-6}<M/M_S<10^3$).** The Einstein angular radius is of the order of the μarcsec.

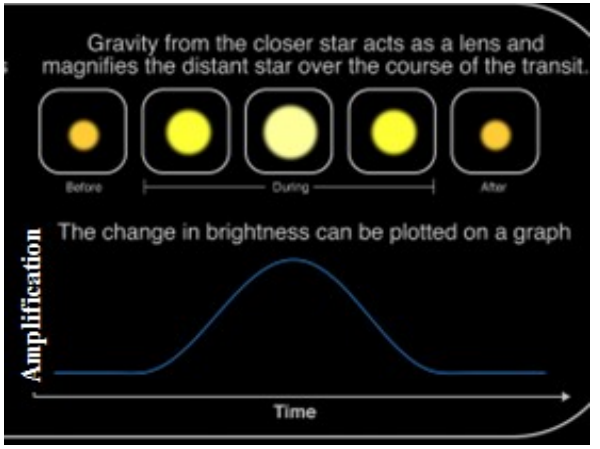

II. GRAVITATIONAL LENSING: Strong lensed quasars

- When a quasar is lensed by foreground galaxies, can be formed multiple images (double, triple or quadruple).
- More than 200 lensed quasars are known:

  Cosmic Lens All Sky Survey (CLASS); Sloan Digital Sky Survey (SDSS)

Future surveys:

Nancy Grace Roman Space Telescope

Vera Rubin Observatory's Legacy Survey of Space and Time (LSST

- By strong lensed quasars can be learn about:
  - Total mass within Einstein radius
  - Mass profile slope ellipticity / orientation
  - can detect /resolve source features
  - Cosmology

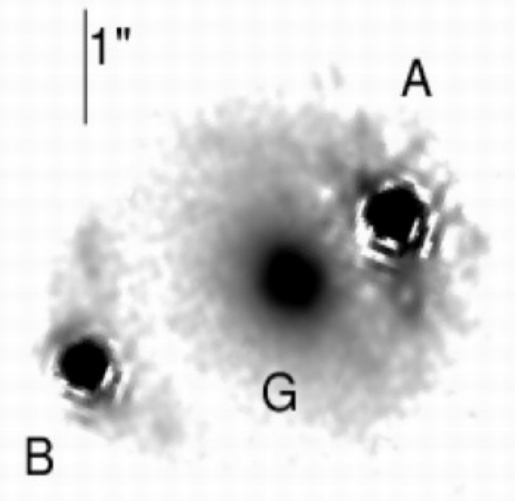

Fig 3. The two-image lens HE1104−1805. G is the lens galaxy and A and B are the quasar images, Z_Q=2.32

II. GRAVITATIONAL LENSING: TIME DELAY

The light ray emitted by source is bending by a lens (galaxy) to arrive the Earth. It needs more time compared to the ray that propagates in empty space for two reasons:

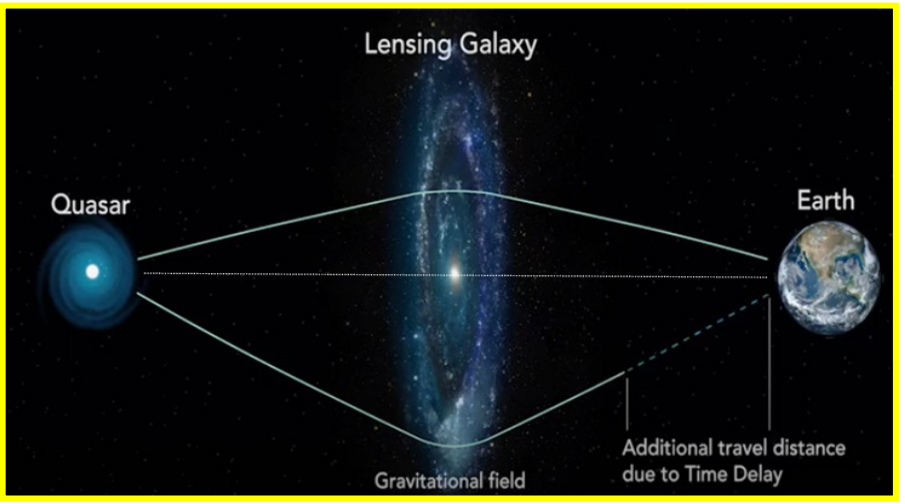

1. bent light ray is longer than a direct one, so need more time to propagate

$$t_{geom} = \frac{1+z_L}{c}\frac{D_L D_S}{D_{LS}}\left[\frac{1}{2}(\vec{\theta}-\vec{\beta})^2\right]$$

2. when light ray propagate through a gravitational potential, happen the time dilation effect (Shapiro delay)

$$t_{grav} = -\frac{1+z_L}{c}\frac{D_L D_S}{D_{LS}}\Psi(\vec{\theta}) + const.$$

$$\Delta t(\vec{\theta}) = \frac{1+z_L}{c}\frac{D_L D_S}{D_{LS}}\left[\frac{1}{2}(\vec{\theta}-\vec{\beta})^2 - \Psi(\vec{\theta})\right] + const$$

$$D_L = \frac{c}{H_0(1+z_L)}\int_0^{z_L}\frac{dz}{E(z)}$$

$$D_S = \frac{c}{H_0(1+z_S)}\int_0^{z_S}\frac{dz}{E(z)}$$

$$D_{LS} = D_S - \frac{1+z_L}{1+z_S}D_L$$

$$E(z) = \sqrt{\Omega_m(1+z)^3 + \Omega_k(1+z)^2 + \Omega_\Lambda}$$

II. GRAVITATIONAL LENSING: TIME DELAY

There are some values of H_0 measured by different methods.

- **Planck flat ΛCMD results suggest an H_0 value lower than other measurements.**
- **Strong time delays are so far in agreement with local estimators but higher than Planck.**

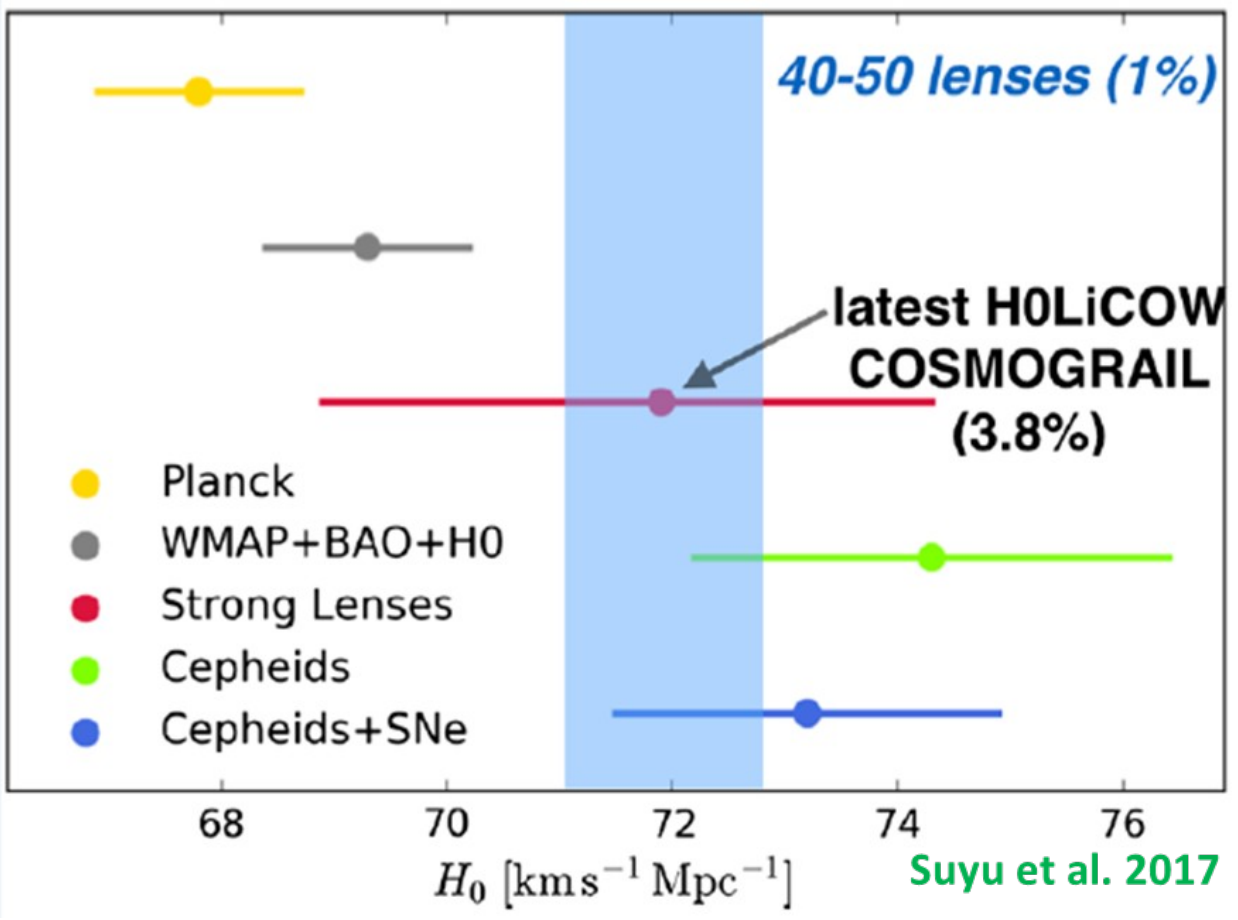

II. GRAVITATIONAL LENSING: TIME DELAY, SIS AND NIS

- **The galaxy mass distribution (Schneider et al. 2006)**

$$\rho = \frac{\sigma_{SIS}^{\ 2}}{2\pi G r^2} \qquad \rho(r) = \frac{\sigma_{SIS}^{\ 2}}{2\pi G}\left(\frac{1}{r^2 + r_c^2}\right)$$

- **By projecting this density along the line of sight, we obtain the surface density and the mass of the lens inside a radius θ from the galactic center in the galactic plane is given by**

$$M(\theta) = \frac{\pi\sigma_{SIS}^{\ 2}}{G}\theta D_L \qquad M(\theta) = \frac{\pi\sigma_{SIS}^{\ 2} D_L}{G}\left(\sqrt{\theta^2 + \theta_c^2} - \theta_c\right)$$

- **Lens potential**

$$\Psi(\theta) = \frac{4\pi\sigma^2}{c^2}\frac{D_{LS}}{D_S}|\theta| \qquad \Psi(\theta) = \theta_0\left[\sqrt{\theta^2 + \theta_c^2} - \theta_c\, ln\left(\sqrt{\theta^2 + \theta_c^2} + \theta_c\right)\right]$$

The algorithm of the quasar lensing

- Generate the redshift of the quasar, following the corresponding distribution;
- Generate the redshift of the galaxy, following the corresponding distributions ; Constrain that the galactic redshift be lower than the quasar redshift. The number of galaxies that fulfilling this condition for each quasar is found by the cumulative number of galaxies ;
- For each generated galaxy, we extract its mass by the stellar mass function and based on the relation between the stellar mass of the galaxy and stellar velocity distribution, find its velocity dispersion;
- Based on the model (SIS) for the galaxies, the galaxy and quasar redshifts, we define the Einstein angle θ_E for the couple quasar/galaxy ;
- Extract a uniformly distributed number n in the interval (0,1) and, considering 200 billions of galaxies in the Universe, keep the couple when $n<10^8 x \theta_E^2/14$ (aligned couple), otherwise reject it (nonaligned couple);
- Repeat the procedure for all expected quasars and keep the predicted aligned couples;;
- For each aligned couple calculate Δt considering SIS and NIS model
- Comparing its θ_E with the resolution of the instrument, estimate the number of lensed quasars expected to be observed by it.

Hamolli et al. 2023

$H_0 = 70\ km\ s^{-1}\ Mpc^{-1}$ $\Omega_m = 0.30$ $\Omega_\Lambda = 0.70$ $\Omega_k = 0$

II. GRAVITATIONAL LENSING: Roman Telescope (NASA)

Scheduled to launch in 2027 at the second Lagrange point (L2) of the Earth-Sun system.

Will observe 2000 square degree of the sky.

Based on the angular resolution of 0.11 arcsec, we find about one in 180 observed quasars will be lensed by the foreground galaxies.

85% of the lensed quasar will be caused by a foreground galaxy.

The most common value of the time delays between the lensed images for both the SIS and the NIS models is around 10 days.

II. GRAVITATIONAL LENSING: microlensing

The image separation is the order of *μarcsec*, so they cannot be resolved, but the total brightness of the images increases with respect to that of the unlensed source and then decreases, leading to a specific time-dependent amplification of the source brightness.

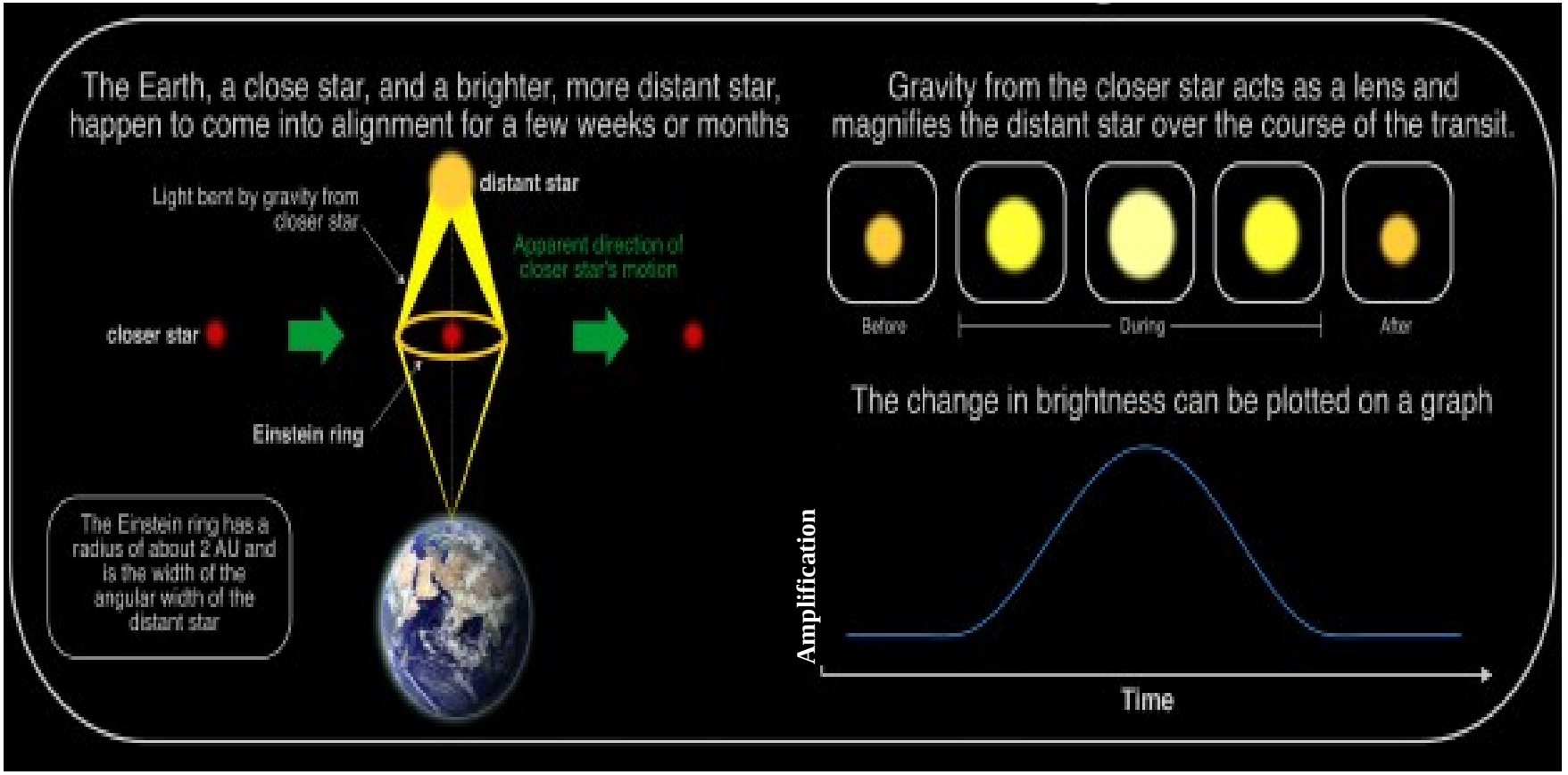

Mroz et al. 2019

- 7 years of observations (2010-2017);
- A sample of 8000 gravitational microlensing events;
- 121 fields located toward the Galactic bulge, covering an area of over 160 deg^2
- Optical Depth.

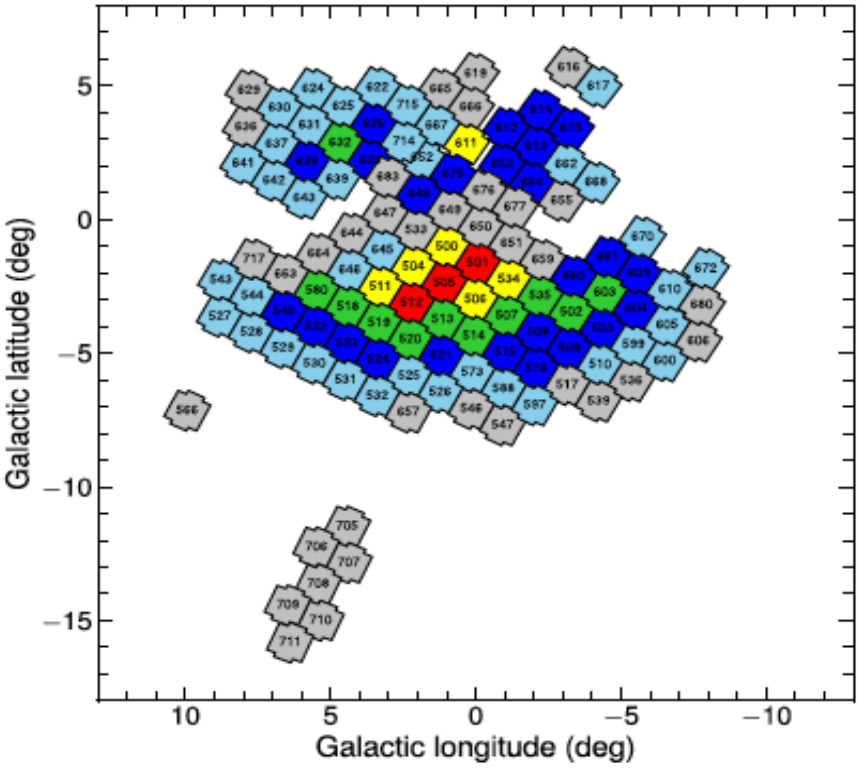

Figure 1. OGLE-IV fields toward the Galactic bulge. Colors mark the typical cadence of observations: red—one observation every 20 minutes, yellow—one observation every 60 minutes, green—two to three observations per night, blue—one observation per night, cyan—one observation per 2 nights. Silver fields were regularly observed during 2010–2013, usually once every 2–3 days.

$$\tau(D_s) = \frac{4\pi G}{c^2} \int_0^{D_s} \rho(D_l) \frac{D_l(D_s - D_l)}{D_s} dD_l$$

$$\tau = \frac{\pi}{2N_* T_{\rm obs}} \sum_i^{N_{\rm ev}} \frac{t_{{\rm E}i}}{\epsilon(t_{{\rm E}i})}$$

Besançon Model

Thin disk

$$\rho_d = \rho_0 \left[\exp\left(-\sqrt{0.25 + \left(\frac{a}{R_d}\right)^2} \right) - \exp\left(-\sqrt{0.25 + \left(\frac{a}{R_h}\right)^2} \right) \right]$$

$$a^2 = r^2 + \left(\frac{z}{\epsilon}\right)^2$$

$$R_d = 2170\ pc$$

$$R_h = 1330\ pc$$

Thick disk

$$\rho(r,z) = \rho_0 \exp\left(\frac{r_\odot - r}{h_R}\right) \begin{cases} 1 - \left(\frac{z^2}{\xi(2h_z+\xi)}\right) & \text{for} \quad z \le \xi \\ \frac{2h_z}{2h_z+\xi} \exp\frac{\xi - |z - z_\odot|}{h_z} & \text{for} \quad z > \xi \end{cases}$$

$$h_z = 533.4\ pc$$

$$h_R = 2355.4\ pc$$

$$\xi = 658\ pc$$

Bar

$$\rho(x,y,z) = \rho_0 \operatorname{sech}^2(-R_s(x,y,z))$$

$$R_s(x,y,z)^{C_\parallel} = \left[\left|\frac{x}{x_0}\right|^{C_\perp} + \left|\frac{y}{y_0}\right|^{C_\perp} \right]^{\frac{C_\parallel}{C_\perp}} + \left|\frac{z}{z_0}\right|^{C_\parallel}$$

$$x_0 = 1.46\ kpc$$

$$y_0 = 0.49\ kpc$$

$$z_0 = 0.3\ kpc$$

$$C_\parallel = 0.5$$

$$C_\perp = 3.007$$

Halo

$$\rho(r,z) = \begin{cases} C_1 a^{-2.44} & \text{for} \quad a > 500\ pc \\ C_1 500^{-2.44} & \text{for} \quad a < 500\ pc \end{cases}$$

$$a = \sqrt{R^2 + \left(\frac{z}{q_{stell}}\right)^2} \qquad q_{stell} = 0.76$$

$$\rho(R_0, 0) = 9.32 \times 10^{-6}\ M_\odot\ pc^{-3}$$

II. GRAVITATIONAL LENSINGOGLE IV observations versus models

Here we compare the observational results with numerical ones, based on theoretical models (Besançon model) for star distributions.

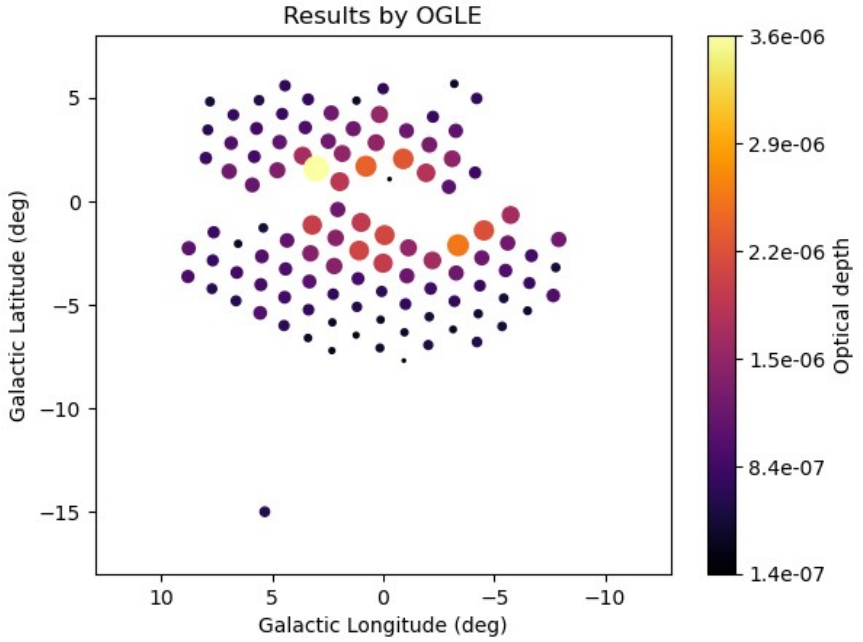

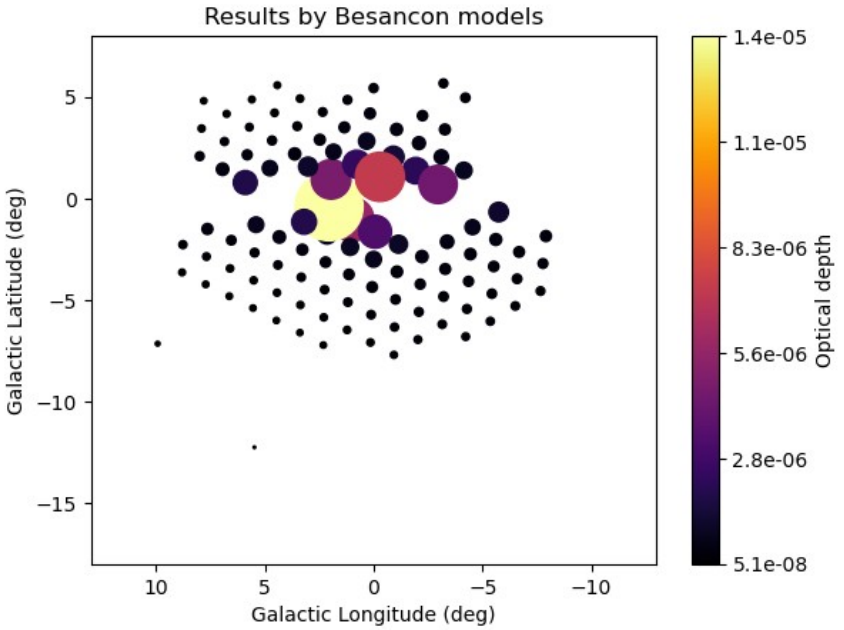

Left: Diagrams with the values of the optical depth, found in 121 channels of OGLE IV observations (colors and surfaces of circles indicate the value)

Right: Numerical values (stars: 7 thin disk and thick disk; bar; halo).

II. GRAVITATIONAL LENSING: OGLE IV observations and the Dark Matter

Here we show the map of the optical depth values for the DM

(OGLE IV observations – numerical values for stars);

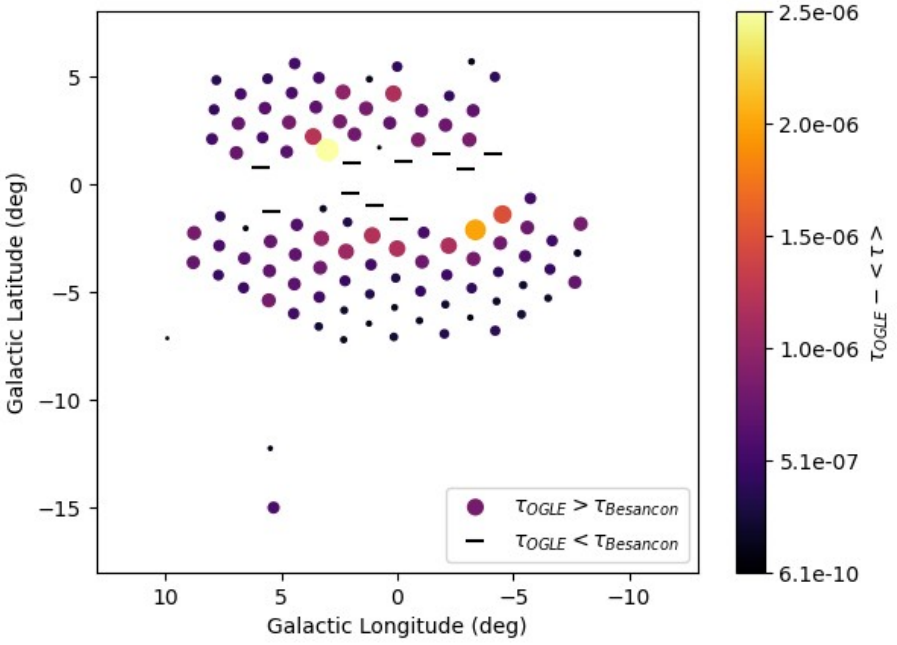

Optical depth of the order of 10^{-6}.

III. GAMMA RAY BURSTS

1. Gamma ray bursts (GRB) are random flashes of gamma radiation, that last from some ms to hundreds of seconds.
2. The prompt emission of gamma ray bursts show complex structures of the observed light curves, but their spectra are more uniform, generally well-fitted by two smoothly connected power-laws.
3. We have been focused on some relations: the lag-luminosity relation, duration-luminosity relation of GRB pulses, peak energy of the spectrum-isotropic energy, peak energy -power-law index of power density spectra and dominant timescale-duration of GRB pulses. These correlations are greatly discussed because they constrain the radiation mechanisms and represent potential distance indicators in Astronomy.

S. Boçi, M. Hafizi, R. Mochkovitch, "The lag and duration-luminosity relations of gamma-ray burst pulses", Astronomy & Astrophysics Vol 519, A76, 2010.

R. Mochkovitch, V. Heussaff, J.L. Atteia, S. Boçi and M. Hafizi, " A simple theory of lags in gamma-ray bursts: Comparison to observations" Astronomy & Astrophysics 592, A95, 2016.

S. Boçi, M. Hafizi, "About some correlations in GRB prompt emission" First Conference organized by the National Institute of Physics (NIP) Academy of Sciences of Albania, 10 - 11 February 2022

IV. DIDACTIC ISSUES

1) On the spatial variation of the magnetic field inside laminar flows of a perfect conductive fluid, the studied cases can be used as complex exercises in an Intermediary course of "Classical Electrodynamics";
2) On the experimental work in conceptual learning of Physics in secondary education in Albania.

B. Duka, S.Boçi "Spatial variation of the magnetic field inside laminar flows of a perfect conductive fluid

V. VERY HOT ACCRETION PLASMA

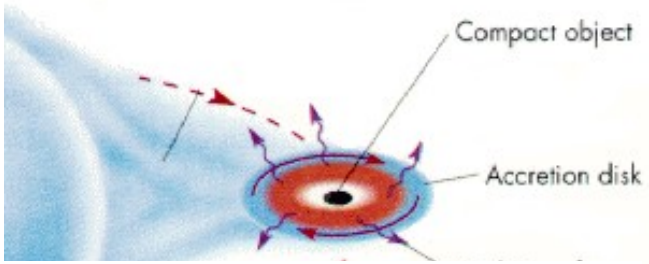

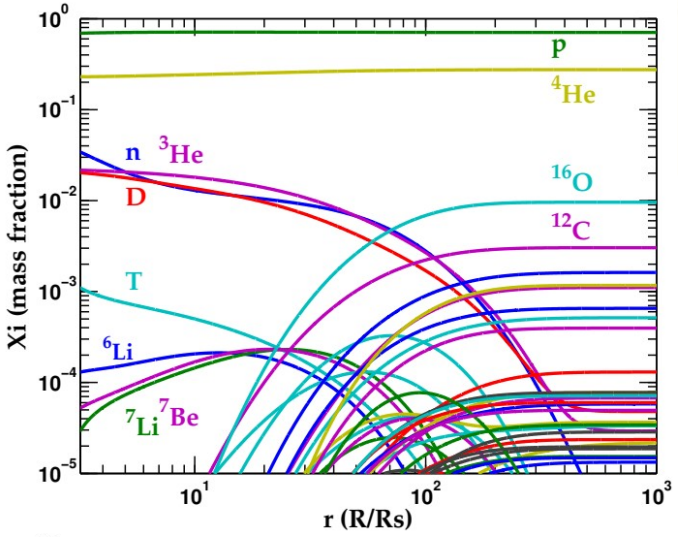

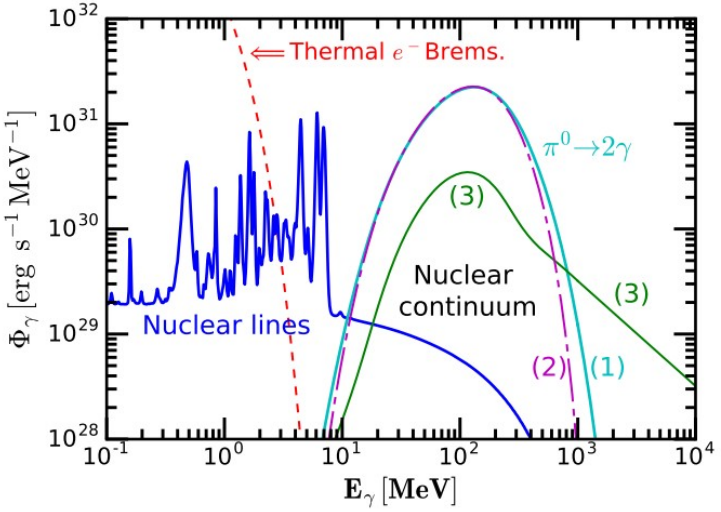

1. **Chemical composition & gamma-ray evolution** of the accretion plasma due to nuclear reactions (e.g. ADAF model).
2. **MeV - GeV gamma-ray emission spectrum** of the accretion plasma resulting from nuclear and hadronic interactions.
3. **Effect of non-fully thermalized** accretion plasma and its effects on the shape of the gamma-ray spectrum.

[e.g: arXiv:1807.06079, arXiv:1201.1729, arXiv:1807.09507]

VI. COSMIC RAY INTERACTIONS

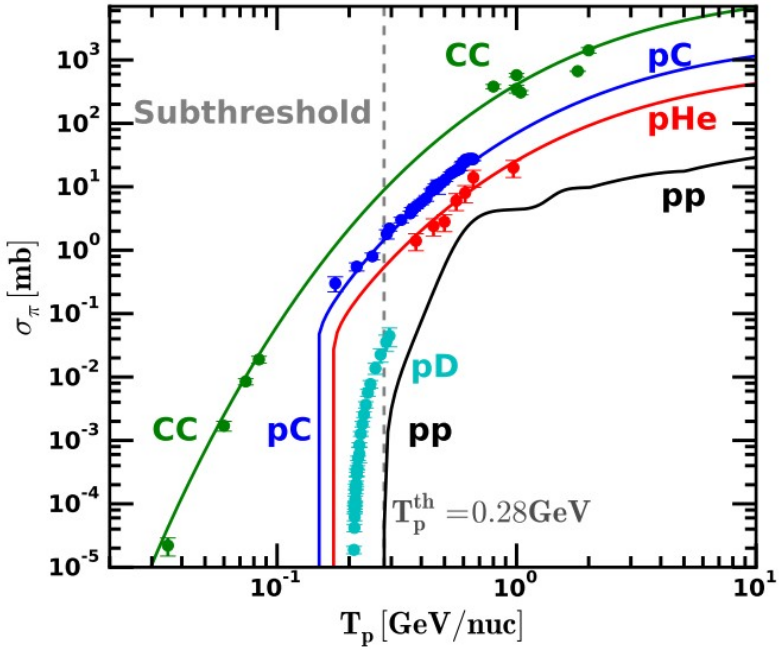

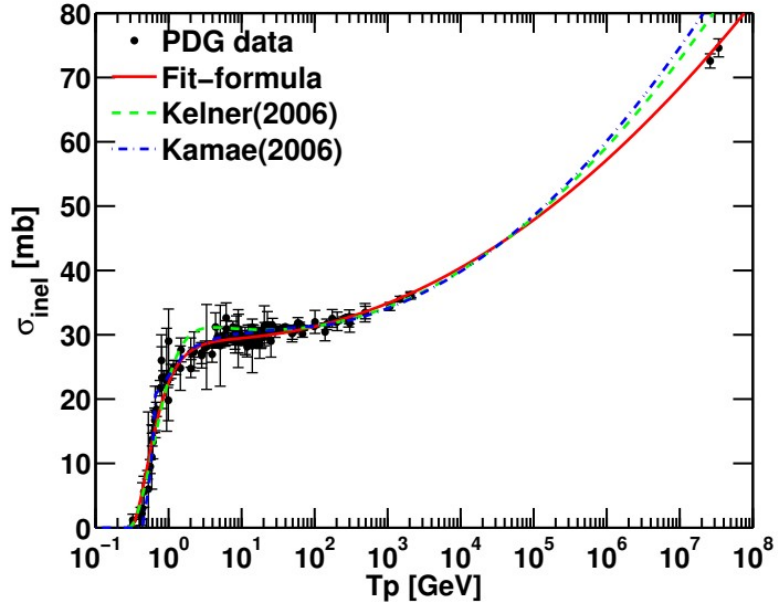

1. **Parametrization p+p, p+A and A+B cross sections**.
2. **Parametrizing multiplicities and differential cross sections** from: Experimental data & Models (Pythia8, QGSJET, Sybill, Epos, etc...)
3. **Production cross sections** for: π, γ, ν, et

[e.g. ..., ..., ...]

Gamma-ray Production Channels

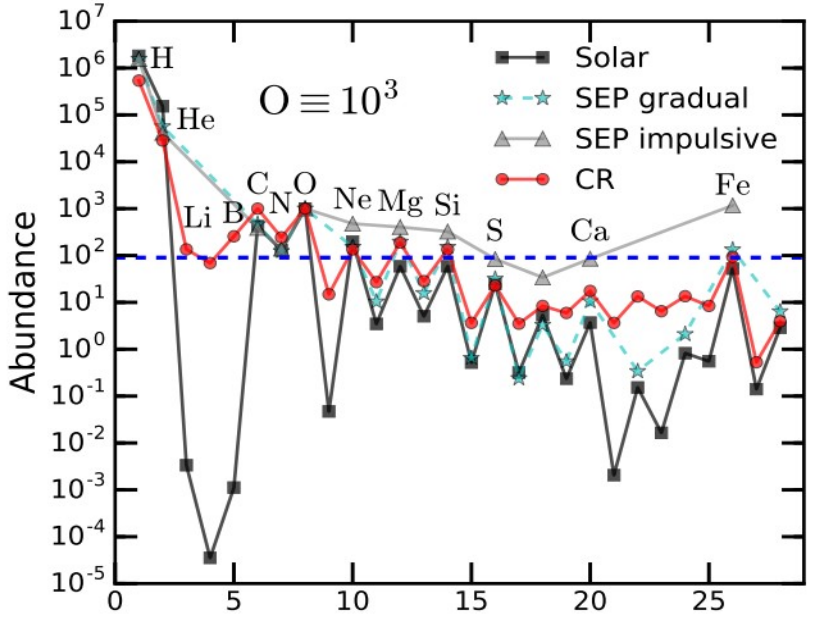

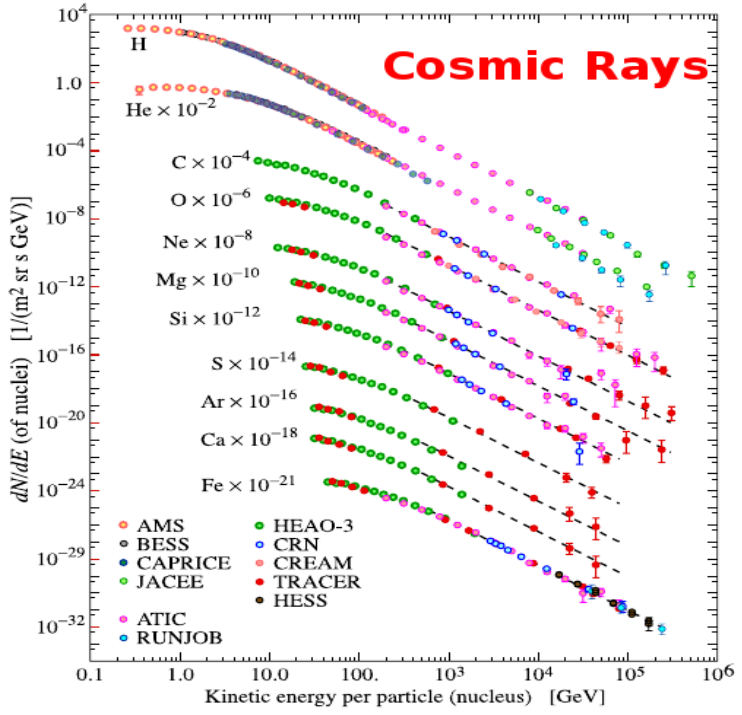

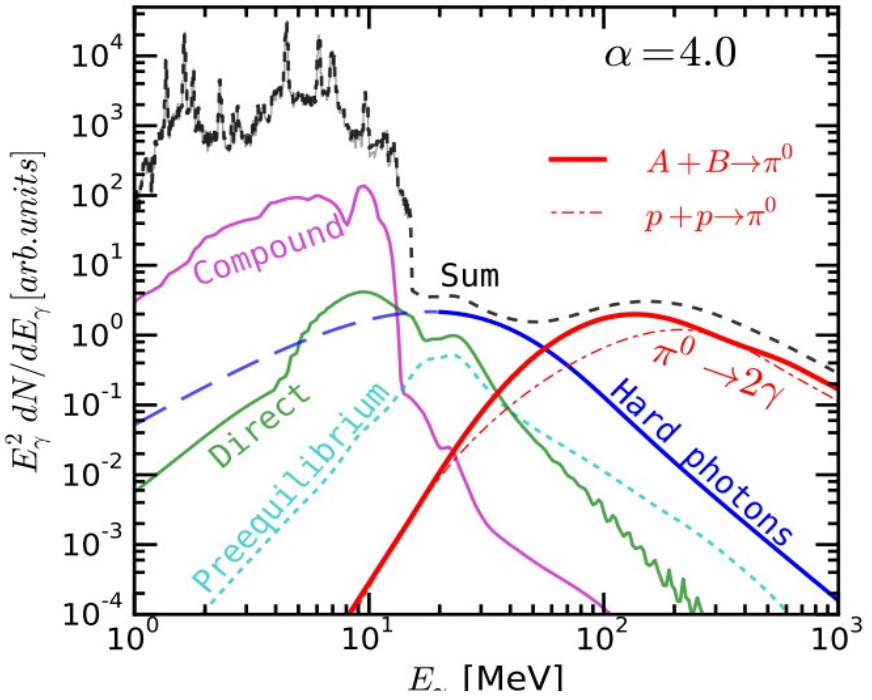

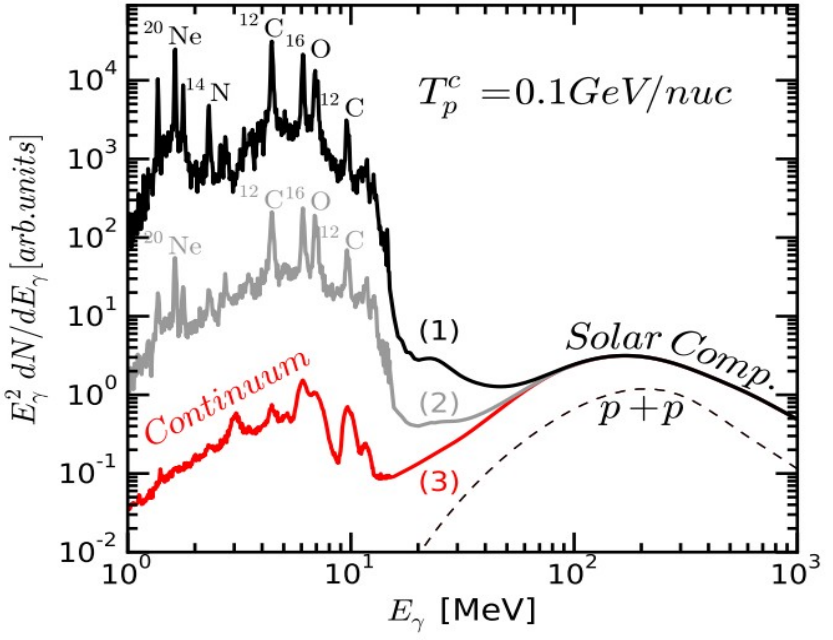

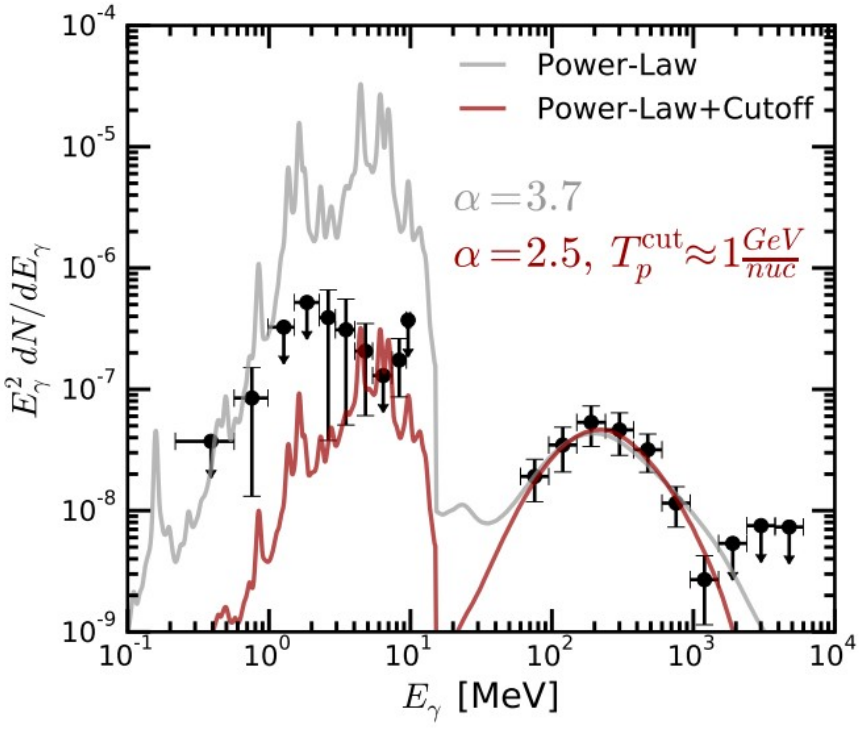

1. Modeling **Solar Flares** gamma-ray emission (Fermi satellite)
2. Modeling **SS433** gamma-ray emission
3. Etc..

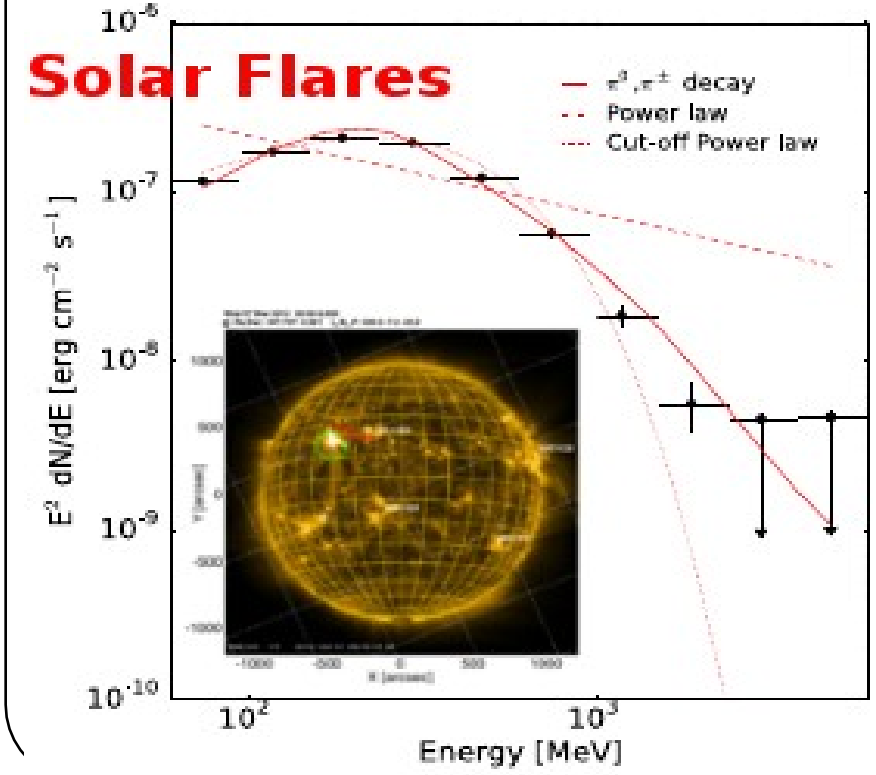

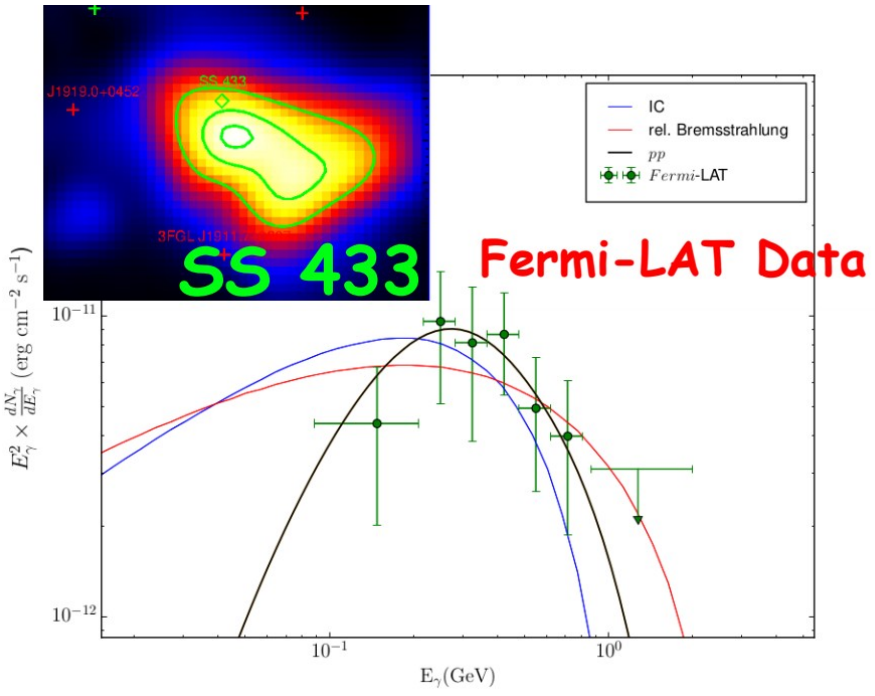

VII. Large High Altitude Air Shower Observatory (LHAASO)

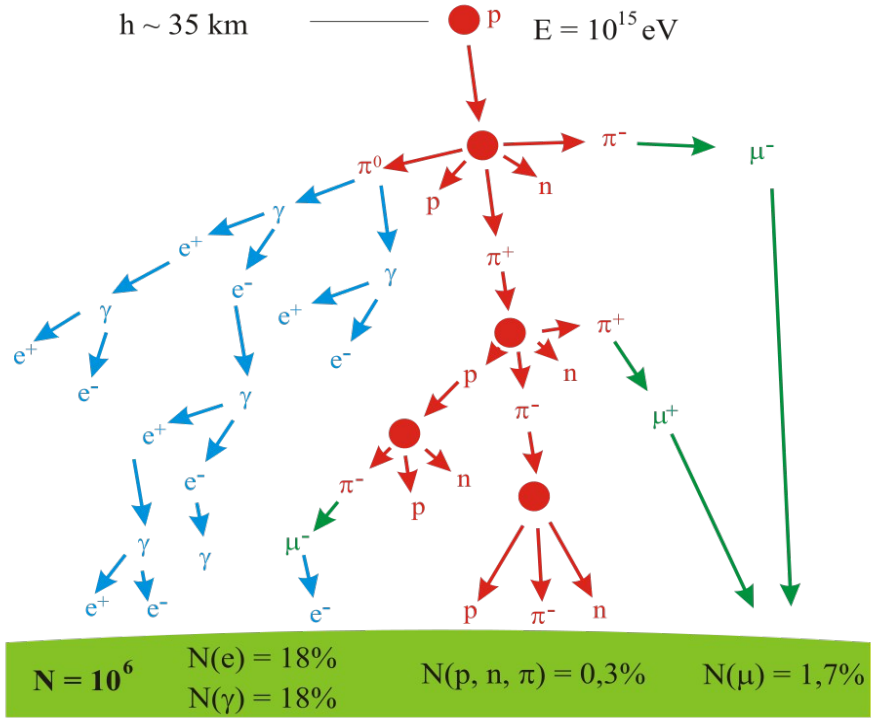

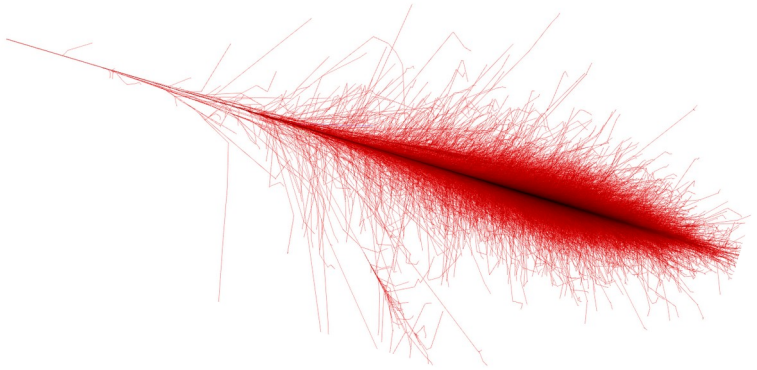

1. Updating and parametrizing secondary particle production cross sections from proton and nuclear interactions

2. Experimental data + Hadronic Models to parametrize the most accurate cross sections for p+p, p+A and A+A interactions

VIII. Detector Simulation

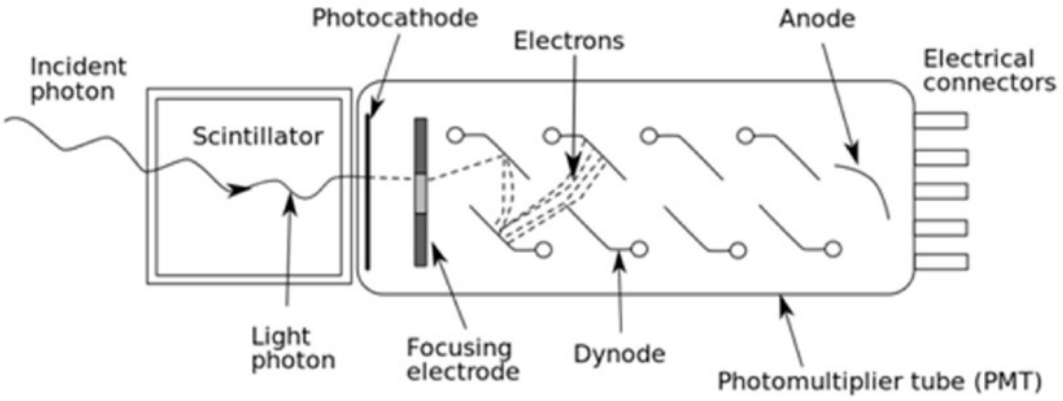

1. Simulation of NaI(Tl) gamma-ray detectors.

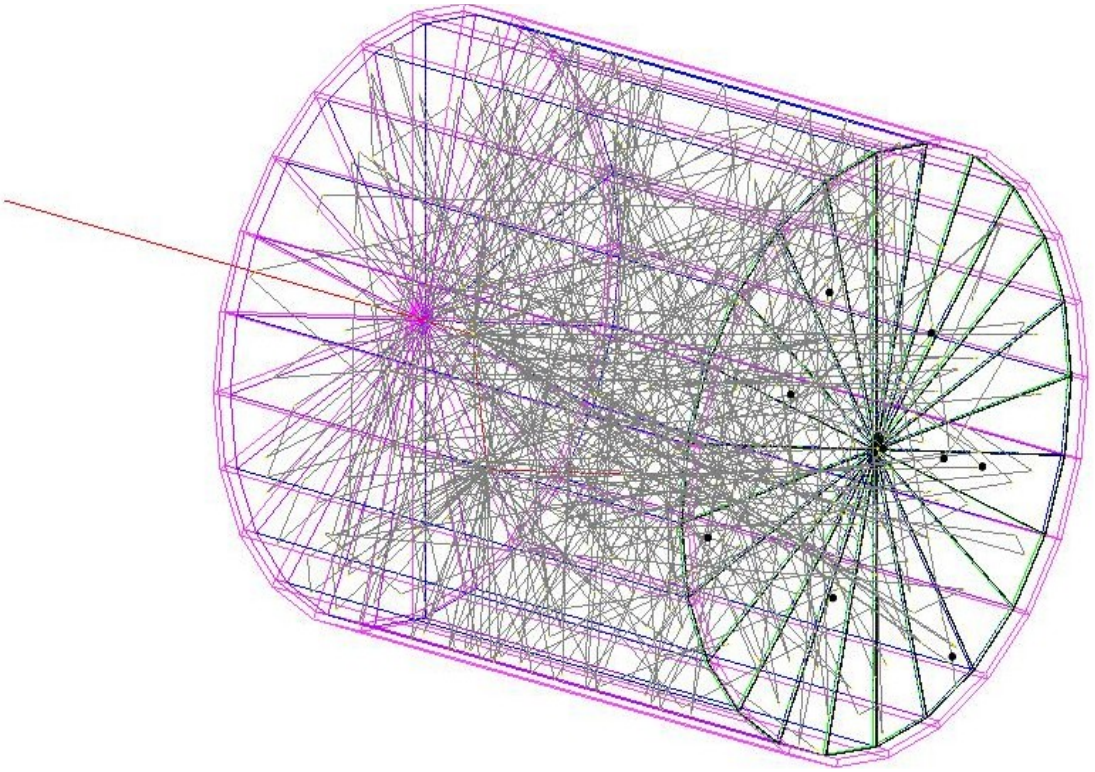

2. Efficiency studies using Geant4